International Journal of Thermodynamics (IJoT)
ISSN 1301-9724 / e-ISSN 2146-1511
https://dergipark.org.tr/en/pub/ijot

Vol. 25 (No. 1), pp. 96-107, 2022
doi: 10.5541/ijot.986170
Published online: March 1, 2022

Thermodynamic Properties of Fluids from Speed of Sound: Integration Along Isentropes

M. Bijedić[1]*, E. Đidić[2]

[1]Faculty of Technology, University of Tuzla, 8 Univerzitetska Str., 75000 Tuzla, Bosnia and Herzegovina
[2]BNT – Factory of Machines and Hydraulics, 1 Mehmeda Spahe Str., 72290 Novi Travnik, Bosnia and Herzegovina
E-mail: [1]muhamed.bijedic@untz.ba [2]enver.dzidic@bnt-tmh.ba

Received 23 August 2021, Revised 25 October 2021, Accepted 1 November 2021

Abstract

The equations connecting speed of sound with other thermodynamic properties of gases and liquids, suitable for numerical integration with respect to temperature, density, and pressure, along isentropes, are derived. Algorithms of their solution are given too. They are tested with several substances (e.g., Ar, N_2, O_2, CH_4, CO_2, and H_2O) in wide ranges of pressure and temperature. Average absolute deviation of thermal properties is 0.0129% in supercritical gaseous phase, 0.0308% in transcritical gaseous phase, and 0.0009% in liquid phase. Corresponding deviations of caloric properties are 0.1706%, 0.1863%, and 0.0702%, respectively.

Keywords: *Thermodynamic properties; fluids; speed of sound, entropy.*

1. Introduction

Thermodynamic properties of gases above their critical temperature may be derived from speed of sound if pressure and temperature, or density and temperature, are used as independent variables. In the former case, initial values of dependent variables (e.g., density and isobaric heat capacity) are specified along the lowest temperature at several pressures. In the later case, initial values of dependent variables (e.g., pressure and isochoric heat capacity) are specified along the lowest temperature at several densities. Numerical integration is performed with respect to temperature in both cases, but along isobars and isochores, respectively. When speed of sound is measured in the same pressure range at each temperature, these data are best exploited if integration is performed along isobars [1, 2]. For initial values specified in the same pressure range, integration along isochores will cover wider pressure range [3]. In this case, initial values may also be specified along the lowest density (e.g., in the limit of ideal gas) at several temperatures, and integration performed with respect to density along isotherms [4]. However, in order to retain stability of the solution, boundary values are needed along the lowest temperature(s). The same sets of initial values may be used to carry out integration below critical temperature. In this case, pressure [2] and density [3, 5] are divided by their corresponding values at saturation, at each temperature, and these quantities are used as new independent variables instead of pressure and density, respectively.

When it comes to liquid phase above critical pressure, temperature and pressure are used as independent variables. Initial values of dependent variables (e.g., density and isobaric heat capacity) are specified along the lowest pressure at several temperatures. Numerical integration is performed with respect to pressure along isotherms [6, 7]. The same set of initial values may be used to carry out integration below critical pressure. In this case integration is performed along paths whose shapes gradually change from that of an isotherm to that of the saturation line [6]. Also, initial values may be specified along the lowest pressure at several temperatures and integration performed along the same paths in opposite direction, or along isotherms with temperature range being extended to the saturation line in each integration step [7]. However, in order to retain stability of the solution in two later approaches, boundary values are needed along the saturation line. Initial values may also be specified along the saturation line and integration performed with respect to pressure along isotherms, but with front of integration having shape of the saturation line rather than that of isobar [6].

If all derivatives appearing in equations connecting speed of sound with other thermodynamic properties (of gases and vapors) are expressed in terms of finite differences [8] or cubic splines [9], the sets of nonlinear algebraic equations are obtained. They can be solved for pressure and heat capacity in very wide ranges of temperature and density. Unlike an approach based on numerical integration, which requires initial values not only of thermal but also of caloric properties (or of thermal ones but of Neumann type), this approach requires only boundary values of thermal properties of Dirichlet type. However, they have to be imposed along overall boundary (e.g., along two isotherms and two isochores).

For initial values specified in the same pressure range, integration along isentropes in gaseous phase will cover wider pressure range than integration along isochores, as one can see from example given at Figure 1. Here, temperature and entropy are used as independent variables.

If density and entropy are used as independent variables, domain of integration could be increased even further, as one can see from example given at Figure 2.

Similarly, for initial values specified in the same temperature range, integration along isentropes in liquid phase will cover wider temperature range than integration

*Corresponding Author

along isotherms, as one can see from example given at Figure 3. Also, isentrope on the left side of integration domain crosses melting line (not seen on the figure) at much higher pressure than corresponding isotherm does. Here, pressure and entropy are used as independent variables.

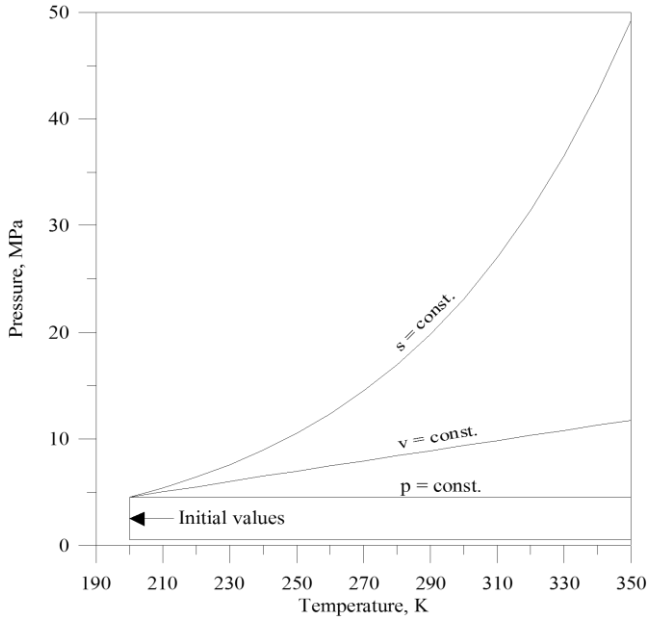

Figure 1. Integration with respect to T at p = const., v = const., and s = const., for methane in gaseous phase [22].

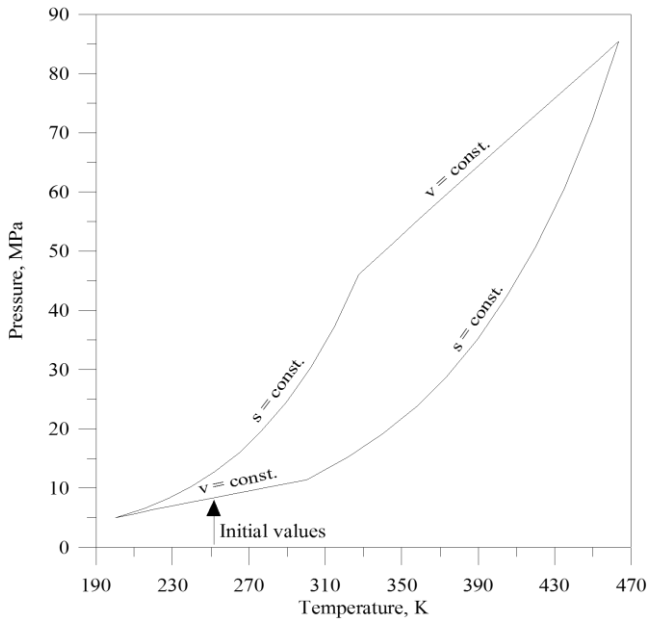

Figure 2. Integration with respect to ρ at s = const., for methane in gaseous phase [22].

Integration with respect to pressure at T = const. in supercritical gaseous phase is not recommended in general, since density increases very quickly with pressure at fixed temperature, and this becomes even more emphasized as critical point is approached. This area of thermodynamic surface could be avoided if integration is conducted at s = const., as one can see from example given at Figure 4.

While entropy is not measurable quantity, it still can be calculated from thermal properties and heat capacity along initial isochore or isobar. Also, it may be used explicitly or implicitly (e.g., in terms of other properties).

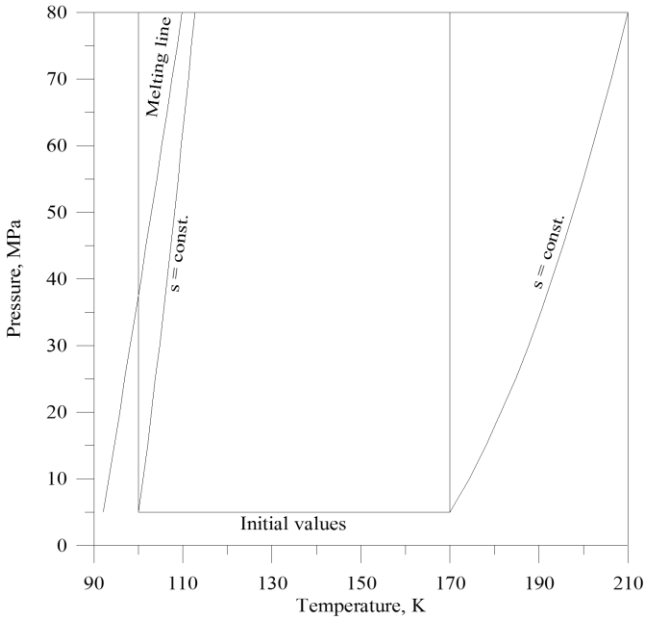

Figure 3. Integration with respect to p at T = const. and s = const., for methane in liquid phase [22].

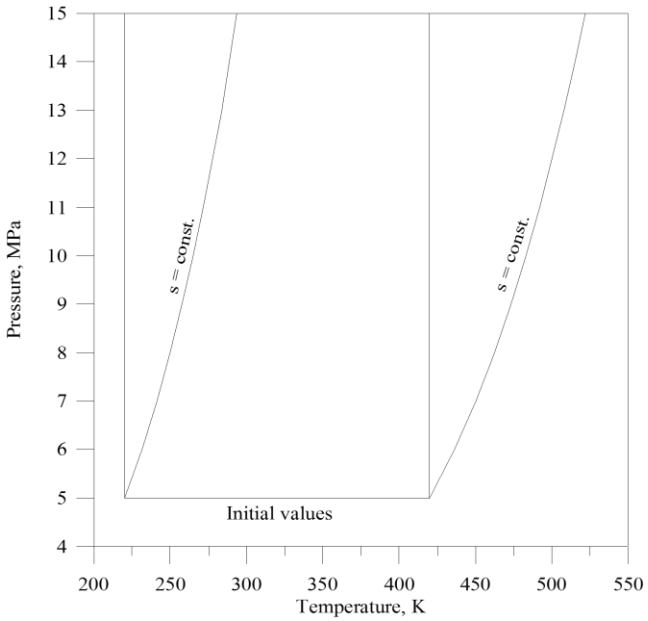

Figure 4. Integration with respect to p at T = const. and s = const., for methane in gaseous phase [22].

2. Theory

The speed of sound is an intensive property whose value depends on the state of the medium through which sound propagates. Experiments indicate that the relation between pressure and density across a sound wave is nearly isentropic. The expression for the speed of sound reads [10]

$$u^2 = \left(\frac{\partial p}{\partial \rho} \right)_s \tag{1}$$

where: u is the speed of sound, p is the pressure, ρ is the mass density, and s is the specific entropy. However, Eq. (1) may not be solved for ρ since u is not measured along isentropes but rather along isotherms. To overcome this, additional property relations have to be included.

2.1 Temperature and entropy as independent variables

2.1.1 Isothermal and isochoric derivatives

According to the following rule of differential calculus

$$\left(\frac{\partial y}{\partial x}\right)_a = \left(\frac{\partial y}{\partial x}\right)_b + \left(\frac{\partial y}{\partial b}\right)_x \left(\frac{\partial b}{\partial x}\right)_a \tag{2}$$

one can write

$$\left(\frac{\partial p}{\partial T}\right)_s = \left(\frac{\partial p}{\partial T}\right)_\rho + \left(\frac{\partial p}{\partial \rho}\right)_T \left(\frac{\partial \rho}{\partial T}\right)_s \tag{3}$$

where T is the thermodynamic temperature. According to another rule

$$\left(\frac{\partial z}{\partial x}\right)_a = \left(\frac{\partial z}{\partial y}\right)_a \left(\frac{\partial y}{\partial x}\right)_a \tag{4}$$

one can also write

$$\left(\frac{\partial p}{\partial T}\right)_s = \left(\frac{\partial p}{\partial \rho}\right)_s \left(\frac{\partial \rho}{\partial T}\right)_s \tag{5}$$

Combining (1), (3), and (5) one obtains

$$\left(\frac{\partial \rho}{\partial T}\right)_s = \left(\frac{\partial p}{\partial T}\right)_\rho \left[u^2 - \left(\frac{\partial p}{\partial \rho}\right)_T\right]^{-1} \tag{6}$$

$$\left(\frac{\partial p}{\partial T}\right)_s = u^2 \left(\frac{\partial \rho}{\partial T}\right)_s \tag{7}$$

If rule (2) is applied to the isochoric derivative in (6), it is obtained

$$\left[\frac{1}{\partial T}\left(\frac{\partial p}{\partial T}\right)_\rho\right]_s = \left(\frac{\partial^2 p}{\partial T^2}\right)_\rho + \frac{\partial^2 p}{\partial T \partial \rho}\left(\frac{\partial \rho}{\partial T}\right)_s \tag{8}$$

The second order isochoric derivative in (8) may be obtained from the following thermodynamic relation [10]

$$\left(\frac{\partial^2 p}{\partial T^2}\right)_\rho = -\frac{\rho^2}{T}\left(\frac{\partial c_v}{\partial \rho}\right)_T \tag{9}$$

where c_v is the specific heat capacity at constant volume, which may be obtained from

$$c_v = \frac{T}{\rho^2}\left(\frac{\partial p}{\partial T}\right)_\rho^2 \left[u^2 - \left(\frac{\partial p}{\partial \rho}\right)_T\right]^{-1} \tag{10}$$

and finally

$$c_p = c_v u^2 \left(\frac{\partial p}{\partial \rho}\right)_T^{-1} \tag{11}$$

where c_p is the specific heat capacity at constant pressure.

2.1.2 Isothermal and isobaric derivatives

According to the rules (2) and (4) one can also write

$$\left(\frac{\partial \rho}{\partial T}\right)_s = \left(\frac{\partial \rho}{\partial T}\right)_p + \left(\frac{\partial \rho}{\partial p}\right)_T \left(\frac{\partial p}{\partial T}\right)_s \tag{12}$$

$$\left(\frac{\partial \rho}{\partial T}\right)_s = \left(\frac{\partial \rho}{\partial p}\right)_s \left(\frac{\partial p}{\partial T}\right)_s \tag{13}$$

Combining (1), (12), and (13) one obtains

$$\left(\frac{\partial p}{\partial T}\right)_s = \left(\frac{\partial \rho}{\partial T}\right)_p \left[\frac{1}{u^2} - \left(\frac{\partial \rho}{\partial p}\right)_T\right]^{-1} \tag{14}$$

$$\left(\frac{\partial \rho}{\partial T}\right)_s = \frac{1}{u^2}\left(\frac{\partial p}{\partial T}\right)_s \tag{15}$$

If rule (2) is applied to the isobaric derivative in (14), it is obtained

$$\left[\frac{1}{\partial T}\left(\frac{\partial \rho}{\partial T}\right)_p\right]_s = \left(\frac{\partial^2 \rho}{\partial T^2}\right)_p + \frac{\partial^2 \rho}{\partial T \partial p}\left(\frac{\partial p}{\partial T}\right)_s \tag{16}$$

The second order isobaric derivative in (16) may be obtained from the following thermodynamic relation [10]

$$\left(\frac{\partial^2 \rho}{\partial T^2}\right)_p = \frac{\rho^2}{T}\left(\frac{\partial c_p}{\partial p}\right)_T + \frac{2}{\rho}\left(\frac{\partial \rho}{\partial T}\right)_p^2 \tag{17}$$

The specific heat capacity at constant pressure may be obtained from

$$c_p = \frac{T}{\rho^2}\left(\frac{\partial \rho}{\partial T}\right)_p^2 \left[\left(\frac{\partial \rho}{\partial p}\right)_T - \frac{1}{u^2}\right]^{-1} \tag{18}$$

and finally

$$c_v = \frac{c_p}{u^2}\left(\frac{\partial \rho}{\partial p}\right)_T^{-1} \tag{19}$$

2.2 Density and entropy as independent variables

2.2.1 Implicit use of entropy

In this case, one can start from the relation [10]

$$\left(\frac{\partial p}{\partial \rho}\right)_s = u^2 \tag{20}$$

and the following property relation [10]

$$\left(\frac{\partial T}{\partial \rho}\right)_s = \frac{1}{\rho^2}\left(\frac{\partial p}{\partial s}\right)_\rho \tag{21}$$

In order to eliminate s at R.H.S. of (21), one can use rule (4) to obtain

$$\left(\frac{\partial p}{\partial s}\right)_\rho = \left(\frac{\partial T}{\partial s}\right)_\rho \left(\frac{\partial p}{\partial T}\right)_\rho \tag{22}$$

If (22) is combined with the following relation [10]

$$c_v = T\left(\frac{\partial s}{\partial T}\right)_\rho \tag{23}$$

it becomes

$$\left(\frac{\partial p}{\partial s}\right)_\rho = \frac{T}{c_v}\left(\frac{\partial p}{\partial T}\right)_\rho \tag{24}$$

Combining (21) and (24) one obtains

$$\left(\frac{\partial T}{\partial \rho}\right)_s = \frac{T}{\rho^2 c_v}\left(\frac{\partial p}{\partial T}\right)_\rho \tag{25}$$

However, Eqs. (20) and (25) may not be solved for p and T since c_v is also unknown. This may be overcome by introducing the following relation [10]

$$\left(\frac{\partial c_v}{\partial \rho}\right)_T = -\frac{T}{\rho^2}\left(\frac{\partial^2 p}{\partial T^2}\right)_\rho \tag{26}$$

Having in mind rule (2) one can write

$$\left(\frac{\partial c_v}{\partial \rho}\right)_s = \left(\frac{\partial c_v}{\partial \rho}\right)_T + \left(\frac{\partial c_v}{\partial T}\right)_\rho \left(\frac{\partial T}{\partial \rho}\right)_s \tag{27}$$

Combining (26) and (27) one obtains

$$\left(\frac{\partial c_v}{\partial \rho}\right)_s = -\frac{T}{\rho^2}\left(\frac{\partial^2 p}{\partial T^2}\right)_\rho + \left(\frac{\partial c_v}{\partial T}\right)_\rho \left(\frac{\partial T}{\partial \rho}\right)_s \tag{28}$$

When c_v is known, c_p may be calculated from

$$c_p = c_v u^2 \left[u^2 - \frac{T}{\rho^2 c_v}\left(\frac{\partial p}{\partial T}\right)_\rho^2\right]^{-1} \tag{29}$$

2.2.2 Explicit use of entropy

In this case, one can also start from the relation [10]

$$\left(\frac{\partial p}{\partial \rho}\right)_s = u^2 \tag{30}$$

and the following property relation [10]

$$\left(\frac{\partial T}{\partial \rho}\right)_s = \frac{1}{\rho^2}\left(\frac{\partial p}{\partial s}\right)_\rho \tag{31}$$

Now, c_v is calculated from [10]

$$c_v = T\left(\frac{\partial T}{\partial s}\right)_\rho^{-1} \tag{32}$$

According to the rule (2), one can write

$$\left(\frac{\partial p}{\partial \rho}\right)_s = \left(\frac{\partial p}{\partial \rho}\right)_T + \left(\frac{\partial p}{\partial T}\right)_\rho \left(\frac{\partial T}{\partial \rho}\right)_s \tag{33}$$

Combining (30), (31), and (33) one obtains

$$\left(\frac{\partial p}{\partial \rho}\right)_T = u^2 - \frac{1}{\rho^2}\left(\frac{\partial p}{\partial s}\right)_\rho \left(\frac{\partial p}{\partial T}\right)_\rho \tag{34}$$

and finally [10]

$$c_p = c_v u^2 \left(\frac{\partial p}{\partial \rho}\right)_T^{-1} \tag{35}$$

2.3 Pressure and entropy as independent variables

In this case, one can start from the relation [10]

$$\left(\frac{\partial \rho}{\partial p}\right)_s = \frac{1}{u^2} \tag{36}$$

and the following property relation [10]

$$\left(\frac{\partial T}{\partial p}\right)_s = -\frac{1}{\rho^2}\left(\frac{\partial \rho}{\partial s}\right)_p \tag{37}$$

In order to eliminate s at R.H.S. of (37), one can use rule (4) to obtain

$$\left(\frac{\partial \rho}{\partial s}\right)_p = \left(\frac{\partial T}{\partial s}\right)_p \left(\frac{\partial \rho}{\partial T}\right)_p \tag{38}$$

If (38) is combined with the following relation [10]

$$c_p = T\left(\frac{\partial s}{\partial T}\right)_p \tag{39}$$

it becomes

$$\left(\frac{\partial \rho}{\partial s}\right)_p = \frac{T}{c_p}\left(\frac{\partial \rho}{\partial T}\right)_p \tag{40}$$

Combining (37) and (40) one obtains

$$\left(\frac{\partial T}{\partial p}\right)_s = -\frac{T}{\rho^2 c_p}\left(\frac{\partial \rho}{\partial T}\right)_p \tag{41}$$

However, Eqs. (36) and (41) may not be solved for ρ and T since c_p is also unknown. This may be overcome by introducing the following relation [10]

$$\left(\frac{\partial c_p}{\partial p}\right)_T = -\frac{T}{\rho^2}\left[\frac{2}{\rho}\left(\frac{\partial \rho}{\partial T}\right)_p^2 - \left(\frac{\partial^2 \rho}{\partial T^2}\right)_p\right] \tag{42}$$

Having in mind rule (2) one can write

$$\left(\frac{\partial c_p}{\partial p}\right)_s = \left(\frac{\partial c_p}{\partial p}\right)_T + \left(\frac{\partial c_p}{\partial T}\right)_p \left(\frac{\partial T}{\partial p}\right)_s \tag{43}$$

Combining (42) and (43) one obtains

$$\left(\frac{\partial c_p}{\partial p}\right)_s = -\frac{T}{\rho^2}\left[\frac{2}{\rho}\left(\frac{\partial \rho}{\partial T}\right)_p^2 - \left(\frac{\partial^2 \rho}{\partial T^2}\right)_p\right] + \left(\frac{\partial c_p}{\partial T}\right)_p \left(\frac{\partial T}{\partial p}\right)_s \tag{44}$$

When c_p is known, c_v may be calculated from

$$c_v = \frac{c_p}{u^2}\left[\frac{1}{u^2} + \frac{T}{\rho^2 c_p}\left(\frac{\partial \rho}{\partial T}\right)_p^2\right]^{-1} \tag{45}$$

3. Algorithms of solution

In this paper it is supposed that practical speed of sound measurements are conducted in p–T domain bounded by two isentropes and two isotherms, isochores, or isobars, respectively, or in any other domain from which speed of sound data can be mapped into the former domains with negligible error. Since true isentropes are yet to be found, approximate ones are generated by a cubic equation of state (EOS). For that purpose the following relation is used

$$s_2 - s_1 = s_2^R - s_1^R + \Delta s^{ig} \tag{46}$$

where entropy change, $s_2 - s_1$, between any two states 1 and 2 is represented as a sum of residual entropy change, $s_2^R - s_1^R$, and ideal gas entropy change Δs^{ig}. The former is obtained from an EOS, while the later is given by

$$\Delta s^{ig} = \int_{T_1}^{T_2} c_p^{ig}(T)\frac{dT}{T} - R\ln\left(\frac{p_2}{p_1}\right) \tag{47}$$

where c_p^{ig} is the ideal gas heat capacity. Since along an isentrope it holds

$$s_2 - s_1 = 0 \tag{48}$$

Eqs. (47) and (48) are replaced into (46), and the resulting equation

$$s_2^R - s_1^R + \int_{T_1}^{T_2} c_p^{ig}(T)\frac{dT}{T} - R\ln\left(\frac{p_2}{p_1}\right) = 0 \tag{49}$$

is solved for p_2 or T_2, given p_1 and T_1. Since Eq. (49) is nonlinear with respect to p_2 and T_2, the solution is obtained by iteration. If u is specified along isotherms or along isochores, specific volume or temperature is iterated, respectively, and pressure is obtained from an EOS directly, since the cubic EOSs are pressure explicit. However, if u is specified along isobars, temperature is iterated in outer loop (finding zero of Eq. (49)), and specific volume in inner loop (finding zero of an EOS).

3.1 Temperature and entropy as independent variables

When it comes to gaseous phase above critical temperature, the most common way of deriving thermodynamic properties from speed of sound is the one based on numerical integration with respect to temperature, along paths of constant density. Although this approach is more demanding (e.g., computationally and experimentally) than the one conducted along paths of constant pressure, it is proved to be more stable. The main source of instability in the later approach are isobaric derivatives, which are estimated less accurately than isochoric ones in the former approach. The aim of the following two algorithms is to check out if isochoric derivatives also introduce less error than isobaric ones when entropy is used instead of density (in the former approach) or pressure (in the latter approach) as independent variable.

3.1.1 Isothermal and isochoric derivatives

1. Specify $u(p, T)$ at several isotherms, along several isentropes generated by a cubic EOS

2. Specify ρ and c_v or $(\partial p/\partial T)_\rho$ at several pressures along isotherm with lowest temperature (T_0)

3. Estimate $(\partial p/\partial \rho)_T$

4. Calculate c_v and c_p from (10) and (11), respectively

5. Estimate $\partial^2 p/\partial T\partial\rho$ and $(\partial c_v/\partial\rho)_T$

6. Calculate $(\partial\rho/\partial T)_s$, $(\partial p/\partial T)_s$, $[\partial(\partial p/\partial T)_\rho/\partial T]_s$, and $(\partial^2 p/\partial T^2)_\rho$ from (6), (7), (8), and (9), respectively

7. Calculate ρ, p, and $(\partial p/\partial T)_\rho$ at $T=T_0+\Delta T$ by numerical integration of (6), (7), and (8), respectively

8. Interpolate EOS pressures along EOS isentropes to T

9. Interpolate u along EOS isentropes to T

10. Interpolate u from EOS pressures to those from step 7

11. Repeat steps 3 to 10 until final temperature is reached

3.1.2 Isothermal and isobaric derivatives

1. Specify $u(p, T)$ at several isotherms, along several isentropes generated by a cubic EOS

2. Specify p and c_p or $(\partial\rho/\partial T)_p$ at several densities along isotherm with lowest temperature (T_0)

3. Estimate $(\partial\rho/\partial p)_T$

4. Calculate c_p and c_v from (18) and (19), respectively

5. Estimate $\partial^2\rho/\partial T\partial p$ and $(\partial c_p/\partial p)_T$

6. Calculate $(\partial p/\partial T)_s$, $(\partial\rho/\partial T)_s$, $[\partial(\partial\rho/\partial T)_p/\partial T]_s$, and $(\partial^2\rho/\partial T^2)_p$ from (14), (15), (16), and (17), respectively

7. Calculate p, ρ, and $(\partial\rho/\partial T)_p$ at $T=T_0+\Delta T$ by numerical integration of (14), (15), and (16), respectively

8. Interpolate EOS pressures along EOS isentropes to T

9. Interpolate u along EOS isentropes to T

10. Interpolate u from EOS pressures to those from step 7

11. Repeat steps 3 to 10 until final temperature is reached

3.2 Density and entropy as independent variables

Thermodynamic properties of gases above their critical temperature may be derived from speed of sound also if numerical integration is conducted with respect to density, along paths of constant temperature. Since this approach requires boundary values along the lowest temperature(s), the aim of the following two algorithms is to check out if the solution is stable without boundary values imposed when integration is conducted along isentropes instead of isotherms. It would be also interesting to compare algorithm which uses entropy explicitly to the one which uses entropy implicitly, because the former solves first order PDEs, while the later solves second order PDEs. Since both temperature and pressure are dependent variables here, it would be also interesting to see if fitted values of speed of sound could successfully replace interpolated ones.

3.2.1 Implicit use of entropy

1. Specify $u(p, T)$ at several isochores and several isentropes generated by a cubic EOS

2. Fit u from step 1 to a suitable function of p and T

3. Specify p and c_v at several temperatures along isochore with lowest density (ρ_0)

4. Estimate $(\partial p/\partial T)_\rho$, $(\partial^2 p/\partial T^2)_\rho$, and $(\partial c_v/\partial T)_\rho$

5. Calculate $(\partial p/\partial \rho)_s$, $(\partial T/\partial \rho)_s$, and $(\partial c_v/\partial \rho)_s$ from (20), (25), and (28), respectively

6. Calculate p, T, and c_v at $\rho=\rho_0+\Delta\rho$ by numerical integration of (20), (25), and (28), respectively

7. Calculate c_p from (29)

8. Calculate u at p and T from step 6 by a function from step 2.

9. Repeat steps 4 to 8 until final density is reached

3.2.2 Explicit use of entropy

1. Specify $u(p, T)$ at several isochores and several isentropes generated by a cubic EOS

2. Fit u from step 1 to a suitable function of p and T

3. Specify p and c_v at several temperatures along isochore with lowest density (ρ_0)

4. Calculate s from (23) along ρ_0, at temperatures from step 3, with initial value chosen arbitrarily

5. Estimate $(\partial p/\partial s)_\rho$ and $(\partial T/\partial s)_\rho$

6. Calculate $(\partial p/\partial T)_\rho = (\partial p/\partial s)_\rho / (\partial T/\partial s)_\rho$

7. Calculate c_v from (32)

8. Calculate $(\partial p/\partial \rho)_T$ from (34)

9. Calculate c_p from (35)

10. Calculate $(\partial p/\partial \rho)_s$ and $(\partial T/\partial \rho)_s$ from (30) and (31), respectively

11. Calculate p and T at $\rho=\rho_0+\Delta\rho$ by numerical integration of (30) and (31), respectively

12. Calculate u at p and T from step 11 by a function from step 2

13. Repeat steps 5 to12 until final density is reached

3.3 Pressure and entropy as independent variables

When thermodynamic properties of liquids are derived from speed of sound, pressure is always used as a variable with respect to which the integration is performed, and the other independent variable is usually temperature. Integration domain is situated between melting line at the left and saturation line at the right, and since these two are not isotherms, significant part of the domain is left uncovered. However, it can be increased considerably if integration is performed along isentropes instead of isotherms. When it comes to gaseous phase, integration with respect to pressure is not stable, even if isothermal paths are replaced by isentropic ones. However, it would be interesting to see if isentropic paths combined with approach similar to the one tried before [9] may solve the problem, especially having in mind aggravating circumstance that boundary values may not be specified along isentrope(s).

3.3.1 Numerical integration

1. Specify $u(p, T)$ at several isobars, along several isentropes generated by a cubic EOS

2. Specify ρ and c_p at several temperatures along isobar with lowest pressure (p_0)

3. Estimate $(\partial \rho/\partial T)_p$, $(\partial^2 \rho/\partial T^2)_p$, and $(\partial c_p/\partial T)_p$

4. Calculate $(\partial \rho/\partial p)_s$, $(\partial T/\partial p)_s$, and $(\partial c_p/\partial p)_s$ from (36), (41), and (44), respectively

5. Calculate ρ, T, and c_p at $p=p_0+\Delta p$ by numerical integration of (36), (41), and (44), respectively

6. Calculate c_v from (45)

7. Interpolate u along EOS isentropes to p

8. Interpolate u from EOS temperatures to those from step 5

9. Repeat steps 3 to 8 until final pressure is reached

3.3.2 Least squares

1. Specify $u(p, T)$ at several isobars, along several isentropes generated by a cubic EOS

2. Specify ρ and c_p at several temperatures along isobar with lowest pressure (p_0)

3. Calculate s from (39) along p_0, at temperatures from step 2, with initial value chosen arbitrarily

4. Guess ρ along isentropes from step 3 at several pressures

5. Estimate $(\partial\rho/\partial p)_s$

6. Calculate u from (36)

7. Interpolate T with respect to u and p

8. Estimate $(\partial T/\partial p)_s$, $(\partial\rho/\partial s)_p$, and $(\partial T/\partial s)_p$

9. Calculate $(\partial\rho/\partial T)_p = (\partial\rho/\partial s)_p / (\partial T/\partial s)_p$

10. Calculate c_p from (39)

11. Calculate c_v from (45)

12. Calculate $f = (\partial T/\partial p)_s + (\partial\rho/\partial s)_p / \rho^2$

13. Calculate $g = (\Sigma f^2) / 2$

14. If $g > 10^{-4}$, calculate new values of ρ by a least squares method

15. Repeat steps 5 to 14 as many times as necessary to obtain $g \leq 10^{-4}$

4. Results and discussion

All interpolations are performed by polynomials [11], while derivatives are estimated by cubic splines [12] and interpolation polynomials. When both pressure and temperature are dependent variables (Algorithms 3.2.1 and 3.2.2), speed of sound data are fitted to bivariate Chebyshev polynomials (with $\ln(p)$ and $\ln(T)$ scaled between -1 and +1). The polynomials coefficients are obtained by method of linear least squares with iterative refinement of Björck [13]. Numerical integrations are performed by Runge-Kutta-Verner fifth-order and sixth-order method with adaptive step-size [14]. In Algorithm 3.3.2, densities are calculated by a modified Levenberg – Marquardt method [15 – 17]. Algorithms of solution described in Sections 3.1 and 3.2 (for gaseous phase) and 3.3 (for liquid and gaseous phase) are tested with several substances. Their list and p–ρ–T ranges covered are given in Tables 1 to 4, 16, 19, and 20. Reference properties are generated by corresponding fundamental EOSs [18 – 24]. Speed of sound data used are obtained from the same EOSs and from measurements [3]. All the results obtained as well as the coefficients of Chebyshev polynomials (see appendix) are given in separate file as a supplement to this paper.

Initial values for supercritical gaseous phase (Algorithms 3.1.1 and 3.1.2) are specified along isotherm with the lowest temperature, at 10 equally spaced pressures (see Table 5). Reference properties are specified at 16 equally spaced isotherms, along 10 isentropes passing through the points with initial values. Speed of sound data are specified at the same isotherms, but along isentropes generated by Peng-Robinson (P-R) EOS [25]. All derivatives are estimated by cubic splines. Both thermal and caloric properties are derived with AADs an order of magnitude smaller if isochoric derivatives are used instead of isobaric ones (see Tables 9 and 10). These AADs are of similar magnitude to those when temperature and density [4] or temperature and pressure [1], respectively, are used as independent variables.

Initial values for supercritical gaseous phase (Algorithms 3.2.1 and 3.2.2) are specified along isochore with the lowest density, at 11 equally spaced temperatures (see Table 6). Entropies corresponding to these temperatures are obtained from Eq. (23), with initial values chosen arbitrarily. Reference properties are specified at 11 isochores, along 11 isentropes passing through the points with initial values. Speed of sound data are specified at isochores and isentropes generated by P-R EOS [25]. Derivatives are estimated by interpolation polynomials (Algorithm 3.2.1) and cubic splines (Algorithm 3.2.2). Both thermal and caloric properties are derived with AADs about 50% smaller if entropy is used explicitly instead of implicitly (see Tables 11 and 12). The solution is stable without boundary values imposed when integration is conducted along isentropes instead of isotherms. Fitted values of speed of sound can successfully replace interpolated ones.

Initial values for transcritical gaseous phase (Algorithms 3.1.1 and 3.1.2) are specified along isotherm with the lowest temperature, at 10 equally spaced pressures (see Table 7). Reference properties are specified at 11 to 15 equally spaced isotherms, along 10 isentropes passing through the points with initial values. Speed of sound data are specified at the same isotherms, but along isentropes generated by P-R EOS [25]. All derivatives are estimated by cubic splines. Both thermal and caloric properties are derived with AADs 4 to 5 times smaller if isochoric derivatives are used instead of isobaric ones (see Tables 13 and 14). These AADs are of similar magnitude to those when temperature and ratio of density to saturated vapor density [5], or temperature and ratio of pressure to saturation pressure [2], respectively, are used as independent variables.

Initial values for liquid phase (Algorithm 3.3.1) are specified along isobar with the lowest pressure, at 7 to 10 equally spaced temperatures (see Table 8). Reference properties are specified at 9 to 11 isobars, along 7 to 10 isentropes passing through the points with initial values. Speed of sound data are specified at the same isobars, but along isentropes generated by P-R EOS [25]. All derivatives are estimated by interpolation polynomials. Both thermal and caloric properties are derived with AADs of similar magnitude to those when pressure and temperature [6, 7] are used as independent variables (see Table 15). It is confirmed that stability of solution in liquid phase, when integration is performed along isentropes, is similar to that along isotherms [26].

Initial values for supercritical gaseous phase (Algorithm 3.3.2) are specified along isobar with the lowest pressure, at 11 equally spaced temperatures (see Table 17). Entropies corresponding to these temperatures are obtained from Eq. (39), with initial values chosen arbitrarily. Reference properties are specified at 11 isobars, along 11 isentropes passing through the points with initial values. Speed of sound data are specified at the same isobars, but along isentropes generated by P-R EOS [25]. All derivatives are estimated by

interpolation polynomials. The results are the same whether guessed values of density are generated by reference EOS (with simulated error of 5%) or by P-R EOS. Both thermal and caloric properties are derived with AADs of similar magnitude to those when density and temperature [4, 9] are used as independent variables (see Table 18). The solution is obtained even without boundary values imposed, but with initial values consisting of thermal and caloric properties.

Initial values for argon in supercritical gaseous phase (Algorithm 3.1.1) are specified along isotherm with the lowest temperature, at 11 equally spaced pressures (see Table 21). Reference properties are specified at 10 isotherms, along 11 isentropes passing through the points with initial values. Speed of sound data [3, 18] are specified at the same isotherms, but along isentropes generated by P-R EOS [25]. All derivatives are estimated by cubic splines. Similar results are obtained with measured and EOS generated speed of sound values, when these later are specified in the same (p, T) points in which speed of sound measurements are conducted (see Table 23).

Initial values for carbon dioxide in transcritical gaseous phase (Algorithm 3.1.1) are specified along isotherm with the lowest temperature, at 8 equally spaced pressures (see Table 22). Reference properties are specified at 9 isotherms, along 9 isentropes passing through the points with initial values. Speed of sound data [3, 23] are specified at the same isotherms, but along isentropes generated by P-R EOS [25]. All derivatives are estimated by cubic splines. Similar results are obtained with measured and EOS generated speed of sound values, when these later are specified in the same (p, T) points in which speed of sound measurements are conducted (see Table 24).

The fact that similar results are obtained with measured and EOS generated speed of sound values, in the last two cases, is confirmation that the two sets of speed of sound have similar uncertainty. So, why AADs in Tables 9 and 23 for argon, or 13 and 24 for carbon dioxide, are an order of magnitude different? This question may be best answered if one takes a closer look at corresponding data sets for argon and carbon dioxide. From Table 1 one can see that temperature range covered for argon is 160 to 310 K and the number of isotherms used is 16, while in Table 20 the corresponding range is 156.08 to 350 K and the number of experimental isotherms is only 10. Also, from Table 3 one can see that temperature range covered for carbon dioxide is 240 to 480 K and the number of isotherms used is 13, while in Table 20 the corresponding range is 250 to 450 K and the number of experimental isotherms is only 6.

5. Conclusions

With only a few initial data, specified at single isotherm, isochore, or isobar, it is possible to derive thermal and caloric properties of real fluids from speed of sound in a wide p–T range if integration paths follow isentropes. While isentropic paths enable covering wider pressure range in gaseous phase, comparing to isochoric paths, this advantage comes at a price. Namely, quicker rise of pressure with temperature along isentropes results in higher nonlinearities, which introduces additional error during interpolation and derivation. It is especially the case when integration is conducted with respect to temperature, but somewhat less pronounced when integration is conducted with respect to density. Besides, selection of appropriate initial temperature and initial pressure range, or initial density and initial temperature range, is of crucial significance if one wants to cover specific area of thermodynamic surface in gaseous phase. Since isentropes of liquids have similar shape to isotherms in p–T coordinates, the solution stability is similar too. However, their positive inclination with respect to isotherms enables wider temperature range to be covered. Generally, the AADs of the results obtained, with respect to corresponding reference data, are such that their uncertainties are similar to those of direct measurements.

Nomenclature

AAD	average absolute deviation (%)
c_p	specific heat capacity at constant pressure (J/kgK)
c_v	specific heat capacity at constant volume (J/kgK)
p	pressure (Pa)
s	specific entropy (J/kgK)
T	thermodynamic temperature (K)
u	speed of sound (m/s)
v	specific volume (m^3/kg)

Greek Letters

ρ	mass density (kg/m^3)

Superscripts

ig	ideal gas
R	residual

Abbreviations

EOS	equation of state
PDE	partial differential equation
P-R	Peng-Robinson

Appendix

Table 1. p–ρ–T ranges covered in supercritical gaseous phase (Algorithms 3.1.1 and 3.1.2).

	p (MPa)		ρ (kg·m^{-3})		T (K)	
	Min	Max	Min	Max	Min	Max
Ar	0.50	29.5246	15.4656	455.7321	160.0	310.0
N_2	0.35	41.5905	8.6420	381.1771	140.0	290.0
O_2	0.50	41.2324	11.6120	457.2604	170.0	320.0
CH_4	0.50	49.2063	4.9837	231.6339	200.0	350.0
CO_2	0.70	35.1821	11.9116	453.9972	320.0	470.0
H_2O	2.20	51.8782	7.4587	218.9286	660.0	810.0

Table 2. p–ρ–T ranges covered in supercritical gaseous phase (Algorithms 3.2.1 and 3.2.2).

	p (MPa)		ρ (kg·m^{-3})		T (K)	
	Min	Max	Min	Max	Min	Max
Ar	5.0	63.5603	243.2643	500.0	160.0	489.4233
N_2	3.5	76.0620	120.9870	375.0	140.0	455.4120
O_2	5.0	73.7194	162.6782	460.0	170.0	470.1185
CH_4	5.0	85.4198	87.76400	240.0	200.0	463.6393
CO_2	7.0	72.2296	178.7401	530.0	320.0	608.2809
H_2O	22.0	98.9995	141.9413	290.0	660.0	957.4060

Table 3. p–ρ–T ranges covered in transcritical gaseous phase (Algorithms 3.1.1 and 3.1.2).

	p (MPa)		ρ (kg·m^{-3})		T (K)	
	Min	Max	Min	Max	Min	Max
Ar	0.1	21.7206	4.0577	252.3890	120.0	400.0
N_2	0.1	33.2891	3.1089	306.9767	110.0	310.0
O_2	0.1	36.8089	3.1174	358.3584	125.0	365.0
CH_4	0.1	48.0311	1.2617	190.7753	155.0	415.0
CO_2	0.1	19.1436	2.2282	240.7653	240.0	480.0
H_2O	0.1	6.9887	0.4738	22.7240	460.0	720.0

Table 4. p–ρ–T ranges covered in liquid phase (Algorithm 3.3.1).

	p (MPa)		ρ (kg·m^{-3})		T (K)	
	Min	Max	Min	Max	Min	Max
Ar	5.0	100.0	1053.233	1495.712	90.0	187.7662
N_2	3.5	90.0	604.0069	917.1604	70.0	158.0081
O_2	5.0	80.0	845.5365	1338.650	60.0	176.0196
CH_4	5.0	80.0	323.9083	469.7829	100.0	209.8933
CO_2	7.0	100.0	914.2519	1253.424	220.0	328.1373
H_2O	0.1	900.0	967.4033	1220.401	280.0	402.2188

Table 5. Points with initial values in supercritical gaseous phase (Algorithms 3.1.1 and 3.1.2).

	p (MPa)			T (K)
	Min	Max	Step	
Ar	0.50	5.0	0.50	160.0
N_2	0.35	3.5	0.35	140.0
O_2	0.50	5.0	0.50	170.0
CH_4	0.50	5.0	0.50	200.0
CO_2	0.70	7.0	0.70	320.0
H_2O	2.20	22.0	2.20	660.0

Table 6. Points with initial values in supercritical gaseous phase (Algorithms 3.2.1 and 3.2.2).

	T (K)			ρ (kg·m^{-3})
	Min	Max	Step	
Ar	160.0	260.0	10.0	243.2643
N_2	140.0	240.0	10.0	120.9870
O_2	170.0	270.0	10.0	162.6782
CH_4	200.0	300.0	10.0	87.76400
CO_2	320.0	420.0	10.0	178.7401
H_2O	660.0	760.0	10.0	141.9413

Table 7. Points with initial values in transcritical gaseous phase (Algorithms 3.1.1 and 3.1.2).

	p (MPa)			T (K)
	Min	Max	Step	
Ar	0.1	1.0	0.1	120.0
N_2	0.1	1.0	0.1	110.0
O_2	0.1	1.0	0.1	125.0
CH_4	0.1	1.0	0.1	155.0
CO_2	0.1	1.0	0.1	240.0
H_2O	0.1	1.0	0.1	460.0

Table 8. Points with initial values in liquid phase (Algorithm 3.3.1).

	T (K)			p (MPa)
	Min	Max	Step	
Ar	90.0	135.0	5.0	5.0
N_2	70.0	115.0	5.0	3.5
O_2	60.0	140.0	10.0	5.0
CH_4	100.0	170.0	10.0	5.0
CO_2	220.0	280.0	10.0	7.0
H_2O	280.0	360.0	10.0	0.1

Table 9. Average absolute deviation in supercritical gaseous phase (Algorithm 3.1.1).

	AAD (%)			
	ρ	p	c_p	c_v
Ar	0.0006	0.0011	0.0080	0.0061
N_2	0.0094	0.0131	0.0709	0.0575
O_2	0.0051	0.0075	0.0516	0.0374
CH_4	0.0057	0.0112	0.0961	0.0671
CO_2	0.0031	0.0041	0.0270	0.0177
H_2O	0.0059	0.0068	0.0629	0.0340

Table 10. Average absolute deviation in supercritical gaseous phase (Algorithm 3.1.2).

	AAD (%)			
	ρ	p	c_p	c_v
Ar	0.0230	0.0431	0.2729	0.1857
N_2	0.0253	0.0383	0.3050	0.2174
O_2	0.0239	0.0352	0.2440	0.1682
CH_4	0.1194	0.1865	1.3816	1.0070
CO_2	0.0275	0.0371	0.2824	0.2234
H_2O	0.0320	0.0399	0.4339	0.3562

Table 11. Average absolute deviation in supercritical gaseous phase (Algorithm 3.2.1).

	AAD (%)			
	p	T	c_p	c_v
Ar	0.0010	0.0033	0.2979	0.1558
N_2	0.0004	0.0014	0.0798	0.0524
O_2	0.0001	0.0004	0.0288	0.0189
CH_4	0.0011	0.0031	0.1798	0.0923
CO_2	0.0002	0.0004	0.0438	0.0299
H_2O	0.0004	0.0010	0.2117	0.1118

Table 12. Average absolute deviation in supercritical gaseous phase (Algorithm 3.2.2).

	AAD (%)			
	p	T	c_p	c_v
Ar	0.0004	0.0010	0.0490	0.0246
N_2	0.0003	0.0012	0.0658	0.0457
O_2	0.0002	0.0011	0.0616	0.0426
CH_4	0.0006	0.0011	0.0780	0.0467
CO_2	0.0003	0.0007	0.0666	0.0463
H_2O	0.0005	0.0011	0.2469	0.1302

Table 13. Average absolute deviation in transcritical gaseous phase (Algorithm 3.1.1).

	AAD (%)			
	ρ	p	c_p	c_v
Ar	0.0071	0.0116	0.0960	0.0663
N_2	0.0031	0.0050	0.0480	0.0306
O_2	0.0138	0.0191	0.1352	0.1030
CH_4	0.0213	0.0285	0.1243	0.0995
CO_2	0.0083	0.0101	0.0739	0.0596
H_2O	0.0016	0.0018	0.0227	0.0212

Table 14. Average absolute deviation in transcritical gaseous phase (Algorithm 3.1.2).

	AAD (%)			
	ρ	p	c_p	c_v
Ar	0.0119	0.0178	0.1032	0.0767
N_2	0.0440	0.0618	0.3475	0.2813
O_2	0.0331	0.0456	0.2994	0.2440
CH_4	0.1575	0.2003	1.0555	0.9065
CO_2	0.0149	0.0175	0.1382	0.1157
H_2O	0.0014	0.0016	0.0128	0.0108

Table 15. Average absolute deviation in liquid phase (Algorithm 3.3.1).

	AAD (%)			
	ρ	T	c_p	c_v
Ar	0.0001	0.0008	0.0603	0.0256
N_2	0.0001	0.0011	0.0839	0.0418
O_2	0.0010	0.0023	0.0759	0.0479
CH_4	0.0002	0.0011	0.0908	0.0507
CO_2	0.0003	0.0019	0.2212	0.1032
H_2O	0.0004	0.0013	0.0229	0.0186

Table 16. p–ρ–T ranges covered in supercritical gaseous phase (Algorithm 3.3.2).

	p (MPa)		ρ (kg·m^{-3})		T (K)	
	Min	Max	Min	Max	Min	Max
Ar	5.0	15.0	63.37348	293.2735	180.0	589.5826
N_2	3.5	14.0	32.52045	204.8415	160.0	535.9944
O_2	5.0	15.0	49.37306	247.1161	190.0	528.8307
CH_4	5.0	15.0	23.28734	122.3224	220.0	521.7476
CO_2	7.0	17.0	70.81165	278.1599	340.0	640.0213
H_2O	22.0	32.0	60.44128	151.0565	680.0	956.5035

Table 17. Points with initial values in supercritical gaseous phase (Algorithm 3.3.2).

	T (K)			p (MPa)
	Min	Max	Step	
Ar	180.0	380.0	20.0	5.0
N_2	160.0	360.0	20.0	3.5
O_2	190.0	390.0	20.0	5.0
CH_4	220.0	420.0	20.0	5.0
CO_2	340.0	540.0	20.0	7.0
H_2O	680.0	880.0	20.0	22.0

Table 18. AAD and number of iterations taken in supercritical gaseous phase (Algorithm 3.3.2).

	Iterations taken	AAD (%)			
		ρ	T	c_p	c_v
Ar	445	0.0007	0.0033	0.1202	0.0847
N_2	334	0.0026	0.0098	0.2915	0.2311
O_2	445	0.0011	0.0032	0.1399	0.1089
CH_4	445	0.0010	0.0015	0.0466	0.0350
CO_2	445	0.0005	0.0018	0.1001	0.0695
H_2O	556	0.0120	0.0133	0.9247	0.2586

Table 19. p–ρ–T ranges covered in supercritical gaseous phase (Algorithm 3.1.1).

	p (MPa)		ρ (kg·m^{-3})		T (K)	
	Min	Max	Min	Max	Min	Max
Ar	0.1	16.5101	3.0975	227.9245	156.08	350.0

Table 20. p–ρ–T ranges covered in transcritical gaseous phase (Algorithm 3.1.1).

	p (MPa)		ρ (kg·m^{-3})		T (K)	
	Min	Max	Min	Max	Min	Max
CO_2	0.5	14.4634	11.0975	198.7124	250.0	450.0

Table 21. Points with initial values in supercritical gaseous phase (Algorithms 3.1.1).

	p (MPa)			T (K)
	Min	Max	Step	
Ar	0.1	2.1	0.2	156.08

Table 22. Points with initial values in transcritical gaseous phase (Algorithms 3.1.1).

	p (MPa)			T (K)
	Min	Max	Step	
CO_2	0.5	1.2	0.1	250.0

Table 23. Average absolute deviation in supercritical gaseous phase (Algorithm 3.1.1).

	AAD (%) using measured speed of sound			
	ρ	p	c_p	c_v
Ar	0.0325	0.0356	0.1198	0.1760
	AAD (%) using EOS generated speed of sound			
Ar	0.0319	0.0351	0.1202	0.1761

Table 24. Average absolute deviation in transcritical gaseous phase (Algorithm 3.1.1).

	AAD (%) using measured speed of sound			
	ρ	p	c_p	c_v
CO_2	0.0845	0.0932	0.5893	0.5254
	AAD (%) using EOS generated speed of sound			
CO_2	0.0340	0.0403	0.3323	0.2874

Chebyshev polynomials in two variables

$$T = \ln\left(T_{i,j}\right)$$

$$P = \ln\left(P_{i,j}\right)$$

$$X_{i,j} = \ln\left(T_{i,j}^{PR}\right)$$

$$Y_{i,j} = \ln\left(P_{i,j}^{PR}\right)$$

$$X = \frac{2T - X_{1,1} - X_{N,N}}{X_{N,N} - X_{1,1}}$$

$$Y = \frac{2P - Y_{1,1} - Y_{N,N}}{Y_{N,N} - Y_{1,1}}$$

$$X_0 = 1$$

$$X_1 = X$$

$$X_2 = 2X^2 - 1$$

$$X_3 = 4X^3 - 3X$$

$$X_4 = 8X^4 - 8X^2 + 1$$

$$X_5 = 16X^5 - 20X^3 + 5X$$

$$X_6 = 32X^6 - 48X^4 + 18X^2 - 1$$

$$X_7 = 64X^7 - 112X^5 + 56X^3 - 7X$$

$$X_8 = 128X^8 - 256X^6 + 160X^4 - 32X^2 + 1$$

$$X_9 = 256X^9 - 576X^7 + 432X^5 - 120X^3 + 9X$$

$$X_{10} = 512X^{10} - 1280X^8 + 1120X^6 - 400X^4 + 50X^2 - 1$$

$$Y_0 = 1$$

$$Y_1 = Y$$

$$Y_2 = 2Y^2 - 1$$

$$Y_3 = 4Y^3 - 3Y$$

$$Y_4 = 8Y^4 - 8Y^2 + 1$$

$$Y_5 = 16Y^5 - 20Y^3 + 5Y$$

$$Y_6 = 32Y^6 - 48Y^4 + 18Y^2 - 1$$

$$Y_7 = 64Y^7 - 112Y^5 + 56Y^3 - 7Y$$

$$Y_8 = 128Y^8 - 256Y^6 + 160Y^4 - 32Y^2 + 1$$

$$Y_9 = 256Y^9 - 576Y^7 + 432Y^5 - 120Y^3 + 9Y$$

$$Y_{10} = 512Y^{10} - 1280Y^8 + 1120Y^6 - 400Y^4 + 50Y^2 - 1$$

$$
\begin{aligned}
U = {} & C_1 + C_2X_1 + C_3Y_1 + C_4X_2 + C_5X_1Y_1 + C_6Y_2 + C_7X_3 \\
& + C_8X_2Y_1 + C_9X_1Y_2 + C_{10}Y_3 + C_{11}X_4 + C_{12}X_3Y_1 \\
& + C_{13}X_2Y_2 + C_{14}X_1Y_3 + C_{15}Y_4 + C_{16}X_5 + C_{17}X_4Y_1 \\
& + C_{18}X_3Y_2 + C_{19}X_2Y_3 + C_{20}X_1Y_4 + C_{21}Y_5 + C_{22}X_6 \\
& + C_{23}X_5Y_1 + C_{24}X_4Y_2 + C_{25}X_3Y_3 + C_{26}X_2Y_4 \\
& + C_{27}X_1Y_5 + C_{28}Y_6 + C_{29}X_7 + C_{30}X_6Y_1 + C_{31}X_5Y_2 \\
& + C_{32}X_4Y_3 + C_{33}X_3Y_4 + C_{34}X_2Y_5 + C_{35}X_1Y_6 \\
& + C_{36}Y_7 + C_{37}X_8 + C_{38}X_7Y_1 + C_{39}X_6Y_2 + C_{40}X_5Y_3 \\
& + C_{41}X_4Y_4 + C_{42}X_3Y_5 + C_{43}X_2Y_6 + C_{44}X_1Y_7 \\
& + C_{45}Y_8 + C_{46}X_9 + C_{47}X_8Y_1 + C_{48}X_7Y_2 + C_{49}X_6Y_3 \\
& + C_{50}X_5Y_4 + C_{51}X_4Y_5 + C_{52}X_3Y_6 + C_{53}X_2Y_7 \\
& + C_{54}X_1Y_8 + C_{55}Y_9 + C_{56}X_{10} + C_{57}X_9Y_1 + C_{58}X_8Y_2 \\
& + C_{59}X_7Y_3 + C_{60}X_6Y_4 + C_{61}X_5Y_5 + C_{62}X_4Y_6 \\
& + C_{63}X_3Y_7 + C_{64}X_2Y_8 + C_{65}X_1Y_9 + C_{66}Y_{10}
\end{aligned}
$$

$T_{i,j}$ calculated temp. at i-th isochore and j-th isentrope
$P_{i,j}$ calculated pressure at i-th isochore and j-th isentrope
$T_{i,j}^{PR}$ temp. at P-R i-th isochore and P-R j-th isentrope
$P_{i,j}^{PR}$ pressure at P-R i-th isochore and P-R j-th isentrope
U speed of sound at $T_{i,j}$ and $P_{i,j}$
C_i coefficients of the Chebyshev polynomial

References:

[1] M. Bijedić, N. Neimarlija, "Thermodynamic Properties of Gases from Speed-of-Sound Measurements," *Int. J. Thermophys.*, *28*, 268-278, 2007.

[2] M. Bijedić, N. Neimarlija, "Thermodynamic Properties of Carbon Dioxide Derived from the Speed of Sound," *J. Iran. Chem. Soc.*, *5*, 286-295, 2008.

[3] Estrada-Alexanders, A. F. (1996). *Thermodynamic Properties of Gases from Measurements of the Speed of Sound* (Doctoral dissertation), Imperial College, London, UK.

[4] M. Bijedić, N. Neimarlija, "Speed of Sound as a Source of Accurate Thermodynamic Properties of Gases," *Lat. Am. Appl. Res.*, *43*, 393-398, 2013.

[5] M. Bijedić, S. Begić, "Thermodynamic Properties of Vapors from Speed of Sound," *J. Thermodyn.*, *2014*, 1-5, 2014.

[6] M. Bijedić, N. Neimarlija, "Thermodynamic Properties of Liquids from Speed of Sound Measurements," *Int. J. Thermodyn.*, *15*, 61-68, 2012.

[7] M. Bijedić, S. Begić, "Density and Heat Capacity of Liquids from Speed of Sound," *J. Thermodyn.*, *2016*, 1-8, 2016.

[8] A. F. Estrada-Alexanders, Justo, D., "New Method for Deriving Accurate Thermodynamic Properties from Speed-of-Sound," *J. Chem. Thermodyn.*, 36, 419-429, 2004.

[9] M. Bijedić, S. Begić, "Solution of the Adiabatic Sound Wave Equation as a Nonlinear Least Squares Problem," *Int. J. Thermophys.*, *40*, 1-36, 2019.

[10] M. J. Moran, H. N. Shapiro, *Fundamentals of Engineering Thermodynamics, 5th Ed.* Chichester: John Wiley & Sons, 2006.

[11] W. Chenney, D. Kincaid, *Numerical Mathematics and Computing, 6th Ed.* Belmont: Thomson Brooks/Cole, 2008.

[12] C. de Boor, *A Practical Guide to Splines.* New York: Springer, 1978.

[13] G. H. Golub, C. F. Van Loan, *Matrix Computations.* Baltimore: Johns Hopkins University Press, 1983.

[14] T. E. Hull, W. H. Enright, and K. R. Jackson, *User's Guide for DVERK – A Subroutine for Solving Non-Stiff ODEs.* University of Toronto, 1976.

[15] K. Levenberg, "A Method for the Solution of Certain Non-Linear Problems in Least Squares," *Q. Appl. Math.*, *2*, 164-168, 1944.

[16] D. Marquardt, "An Algorithm for Least-Squares Estimation of Nonlinear Parameters," *SIAM J. Appl. Math.*, *11*, 431-441, 1963.

[17] J.J. Moré, B.S. Garbow, and K.E. Hillstrom, *User Guide for MINPACK-1*. Argonne National Laboratory Report ANL-80-74, 1980.

[18] C. Tegeler, R. Span, and W. Wagner, "A New Equation of State for Argon Covering the Fluid Region for Temperature from the Melting Line to 700 K at Pressures up to 1000 MPa," *J. Phys. Chem. Ref. Data*, *28*, 779-850, 1999.

[19] R. Span, E. W. Lemmon, R. T. Jacobsen, W. Wagner, and A. Yokozeki, "A Reference Equation of State for the Thermodynamic Properties of Nitrogen Covering the Fluid Region for Temperatures from 63.151 to 1000 K and Pressures to 2200 MPa," *J. Phys. Chem. Ref. Data*, *29*, 1361-1433, 2000.

[20] R. Schmidt, W. Wagner, "A New Form of the Equation of State for Pure Substances and Its Application to Oxygen," *Fluid Phase Equilibria*, *19*, 175-200, 1985.

[21] R. B. Stewart, R. T. Jacobsen, and W. Wagner, "Thermodynamic Properties of Oxygen from the Triple Point to 300 K with Pressures to 80 MPa," *J. Phys. Chem. Ref. Data*, *20*, 917-1021, 1991.

[22] U. Setzmann, W. Wagner, "A New Equation of State and Tables of Thermodynamic Properties for Methane Covering the Range from the Melting Line to 625 K and Pressures up to 1000 MPa," *J. Phys. Chem. Ref. Data*, *20*, 1061-1125, 1991.

[23] R. Span, W. Wagner, "A New Equation of State for Carbon Dioxide Covering the Fluid Region for Temperature from the Triple-Point Temperature to 1100 K at Pressures up to 800 MPa," *J. Phys. Chem. Ref. Data*, *25*, 1509-1596, 1996.

[24] W. Wagner, A. Pruss, "The IAPWS Formulation 1995 for the Thermodynamic Properties of Ordinary Water Substance for General and Scientific Use," *J. Phys. Chem. Ref. Data*, *31*, 387-535, 2002.

[25] D. Y. Peng, D. B. Robinson, "A New Two-Constant Equation of State," *Ind. Eng. Chem. Fund.*, *15*, 59-64, 1976.

[26] S. Lago, P. A. Giuliano Albo, "A Recursive Equation Method for the Determination of Density and Heat Capacity: Comparison Between Isentropic and Isothermal Integration Paths," *J. Chem. Thermodyn.*, *42*, 462-465, 2010.